Analysis of the General Circulation of the Atmosphere Through Low- and Mid-Latitude Phenomena

Vince Agard

May 2009

Abstract

In this study, the overall circulatory patterns of the Earth's atmosphere are examined through laboratory experimentation and analysis of meteorological data. Specifically, the mechanisms through which heat is transferred poleward from the tropics are examined. The Hadley circulation and mid-latitude eddies are analyzed using conservation of angular momentum, thermal wind balance, and balance of heat fluxes. It is concluded that the patterns composing the general circulation of the atmosphere contribute effectively to a net poleward heat flux, and that the conducted laboratory experiments are analogous to these atmospheric processes.

1 Introduction

While solar radiation is the primary source of heat for the Earth's atmosphere, the spherical nature of the Earth's surface in conjunction with the relatively large distance between Sun and Earth means that a disproportionate amount of the total solar energy striking the Earth falls in the tropics. While there is an observed temperature gradient between equator and pole, with no meridional heat transport this temperature difference would be much greater. In fact, it is implied that there must be almost 6 petawatts (6×10^{15} watts) of poleward heat transport to sustain the observed meridional temperature gradient (Marshall & Plumb, 2008). This study aims to understand the mechanisms in the general circulation of the Earth's atmosphere that contribute to this heat transport.

Circulational phenomena in the atmosphere are responsible for a significant amount of this meridional heat transport. At low latitudes, Hadley cells compose a large-scale overturning meridional circulation, with upwelling and deep convection near the equator, and dry subsidence in subtropical regions. Meanwhile, in mid-latitudes, turbulent flow is present as transient eddies travel throughout the atmosphere.

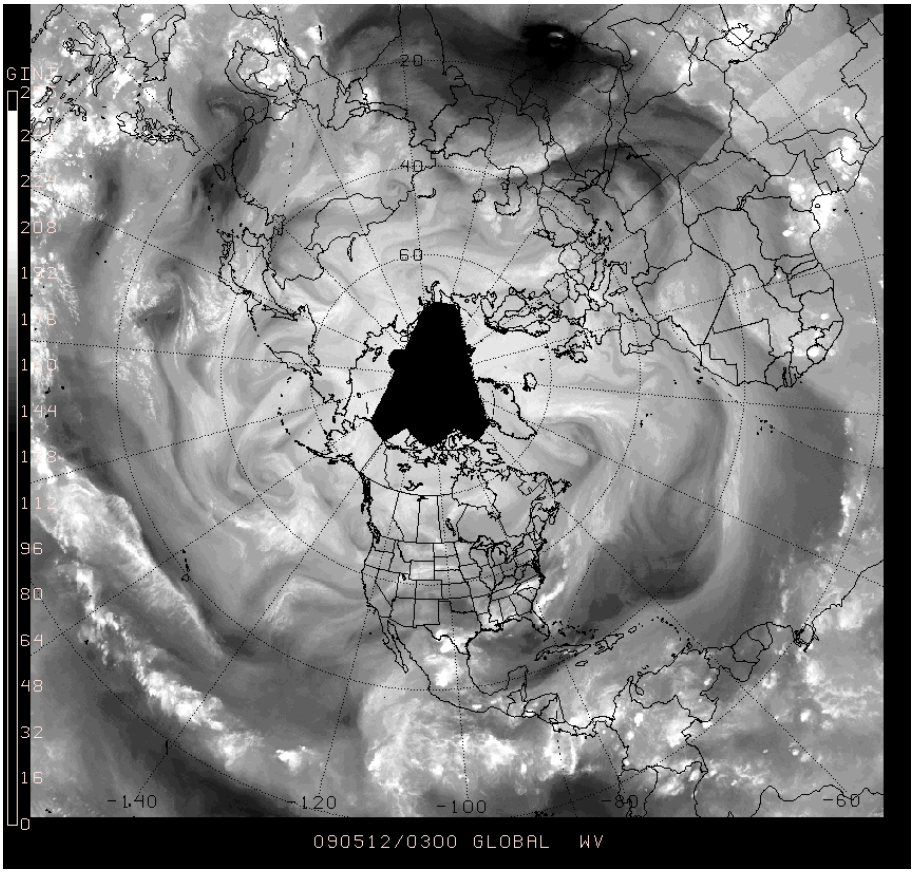

Figure 1: An instantaneous satellite water vapor image of the northern hemisphere on May 12, 2009 (PSU).

These phenomena can be observed in Fig. 1, as an instantaneous satellite water vapor image of the northern hemisphere shows eddy flow at mid-latitudes closer to the pole, followed when by a band of dry air further from the pole, and finally a band of convective storms near the equator. Further investigation of the Hadley circulation and mid-latitude eddies can yield more information about their contributions to meridional heat transport.

2 Low latitudes: The Hadley circulation

In the absence of rotation, the temperature-driven meridional circulation would consist of upwelling of warm air at low latitudes and meridional transport of warm air to high latitudes, followed by subsidence at high latitudes and return flow of cold air along the surface (Illari &

Marshall, 2009). Indeed, at low latitudes, the Earth's surface is nearly parallel to its axis of rotation, and therefore the effects of rotation are weakly felt. Present at these low latitudes, the Hadley circulation is a meridional overturning circulation similar to that which would exist in the absence of rotation.

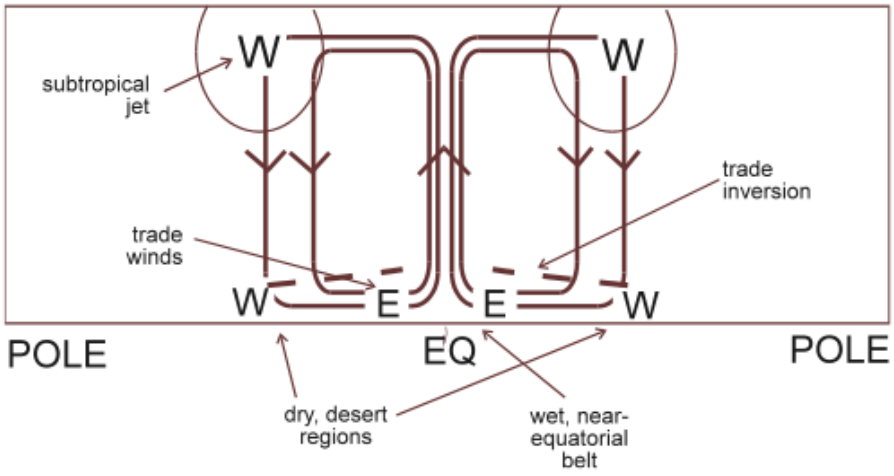

Figure 2: Schematic of a typical Hadley circulation in the tropics. Westerlies are marked 'W', and easterlies are marked 'E'. Arrows indicate direction of air flow (Illari & Marshall, 2009).

A schematic of the Hadley circulation is shown in Fig. 2. Near the equator, tropical Hadley cells feature deep convection in a region known as the Intertropical Convergence Zone (ITCZ), where converging surface winds create a region of warm air upwelling. Having risen to the top of the troposphere, this warm air then diverges poleward to the north and south. However, as air parcels gain latitude, they move closer to the Earth's axis of rotation. Conservation of angular momentum dictates that their zonal speed must therefore increase. As air parcels just below the tropopause move poleward, they therefore build westerly wind speed, and westerly subtropical jets are formed at approximately 30 degrees latitude, where subsidence occurs. Since the subsiding air parcels have little or no moisture, the regions in which subsidence occurs are very dry, and sometimes contain deserts. Finally, cooler air returns to the equatorial region along the surface. As the air moves equatorward, it moves away from the axis of rotation of the Earth, and conservation of angular momentum therefore dictates that these air parcels gain an easterly zonal velocity. These easterly tropical surface winds are known as the tradewinds. Finally, the tradewinds converge once again in the ITCZ, resulting in upwelling and completing the Hadley cycle.

The westerly jets associated with the Hadley circulation are also consistent with thermal

wind balance, in which a vertical wind shear is proportional to horizontal temperature gradients. Indeed, the vertical wind shear present at the edge of the Hadley cell at which large westerly jets are present is associated with a meridional temperature gradient. Here, there is a contrast between warm, well-mixed air in the tropics and cooler air in mid-latitudes. The resulting temperature gradient is generally located at the same latitude as the westerly jets in the Hadley circulation. This thermal wind relationship can be observed through atmospheric data in which the overall nature of the Hadley circulation can be determined.

2.1 Climatological Hadley cell data analysis

To investigate the Hadley circulation in the atmosphere, long-term climatological temperature and wind data were analyzed for both northern and southern summer. For the months of January and July, zonally-averaged profiles were generated showing the climatological mean of each variable from 1948 to present. The data examined included temperature, as well as the zonal, meridional, and vertical components of wind.

Fig. 3 shows a climatological latitude-height profile of temperature, overlaid with climatological zonal wind data. Meanwhile, Figs. 4 and 5 show climatological profiles of vertical air velocity in January and July, while Figs. 6 and 7 show profiles of meridional air velocity for the same times.

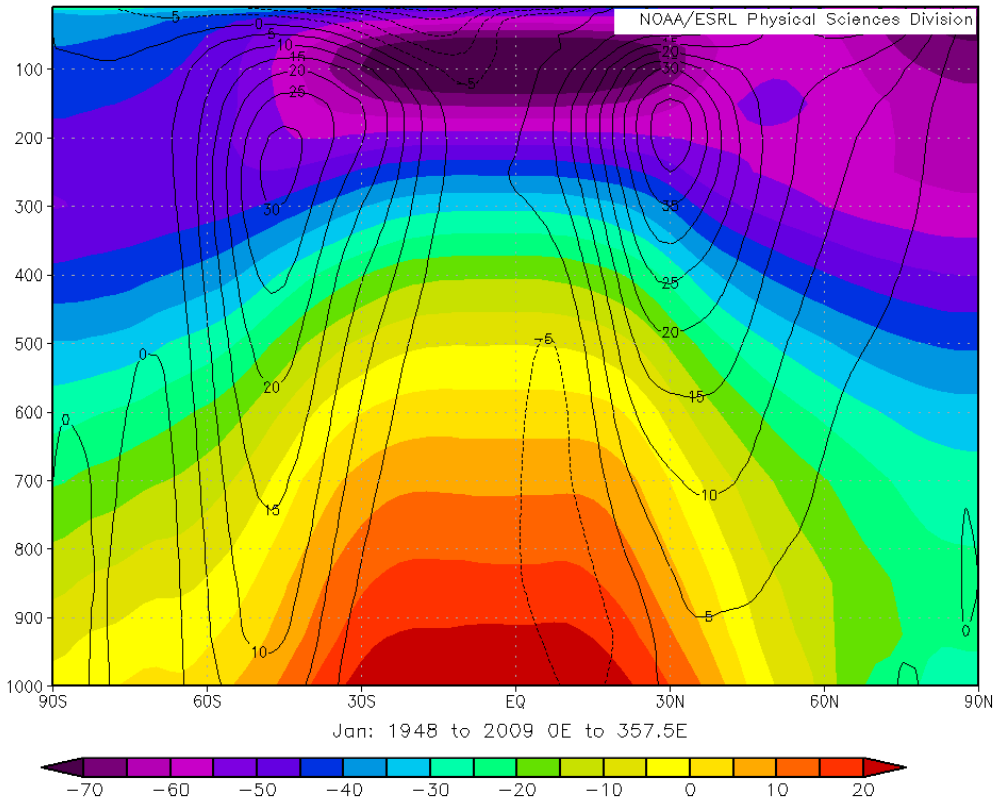

Figure 3: Zonally-averaged temperature (shaded colors, in units of °C) and zonal wind (black contours, in units of m/s) data are plotted in a latitude-height profile. These data represent a climatological average for the month of January over the years 1948-2009 (ESRL).

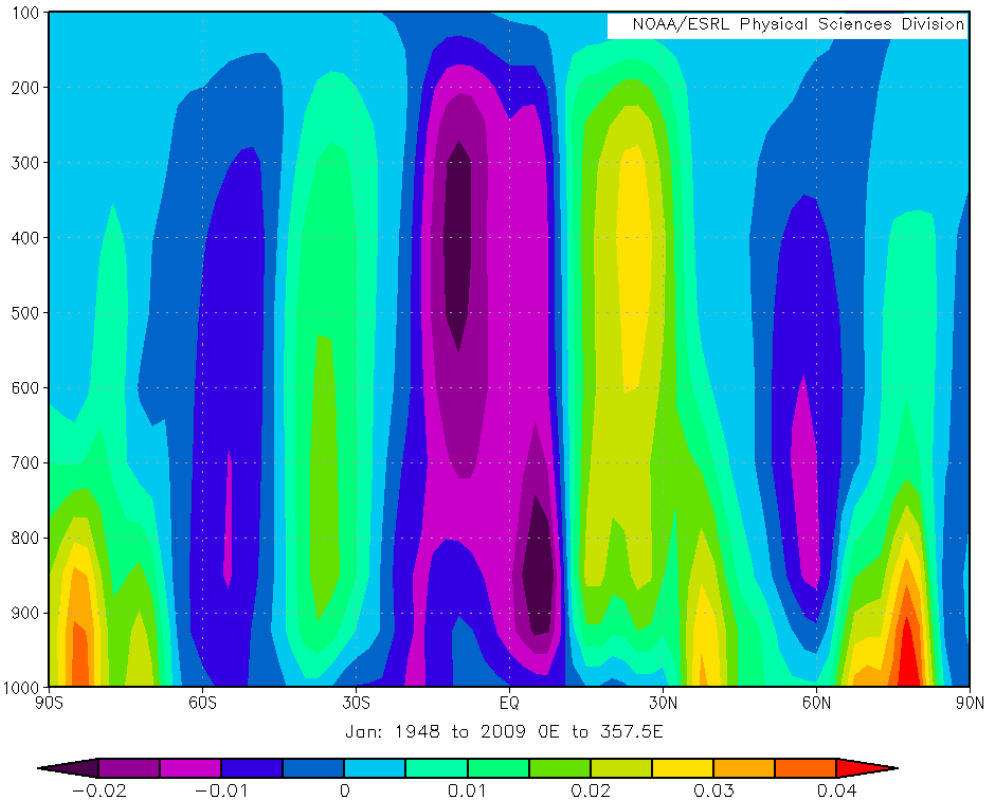

Figure 4: Zonally-averaged vertical velocity data (in units of Pa/s) are plotted in a latitude-height profile. These data represent a climatological average for the month of January over the years 1948-2009 (ESRL).

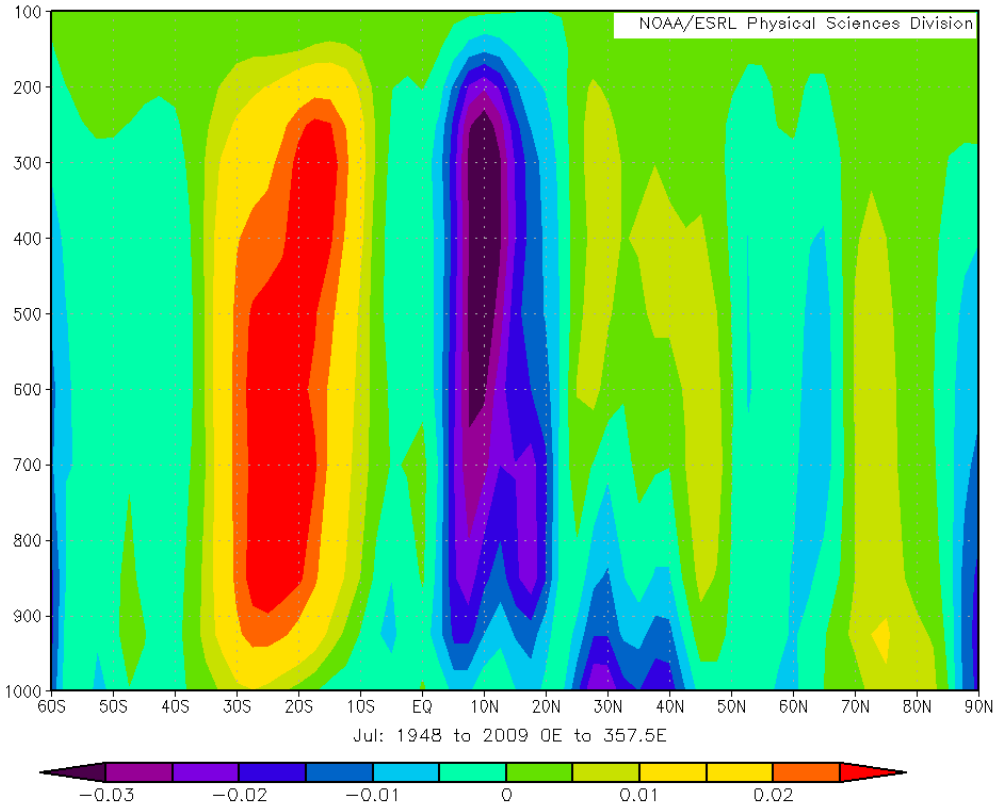

Figure 5: Zonally-averaged vertical velocity data (in units of Pa/s) are plotted in a latitude-height profile. These data represent a climatological average for the month of July over the years 1948-2009 (ESRL).

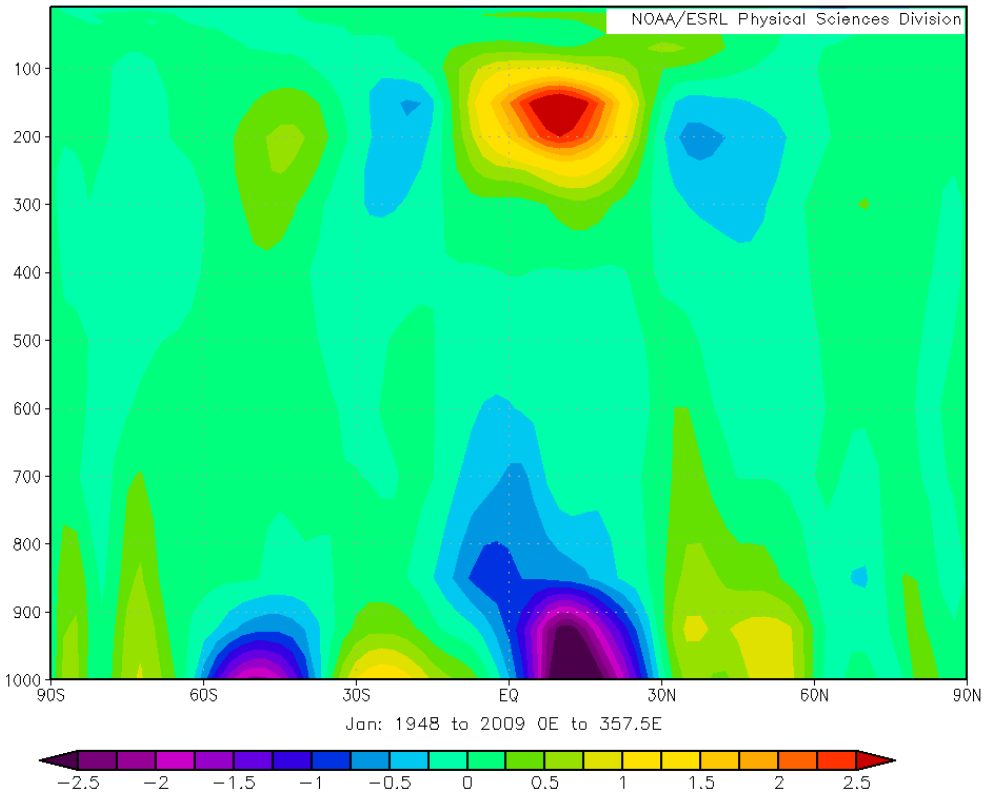

Figure 6: Zonally-averaged zonal velocity data (in units of m/s) are plotted in a latitude-height profile. These data represent a climatological average for the month of January over the years 1948-2009 (ESRL).

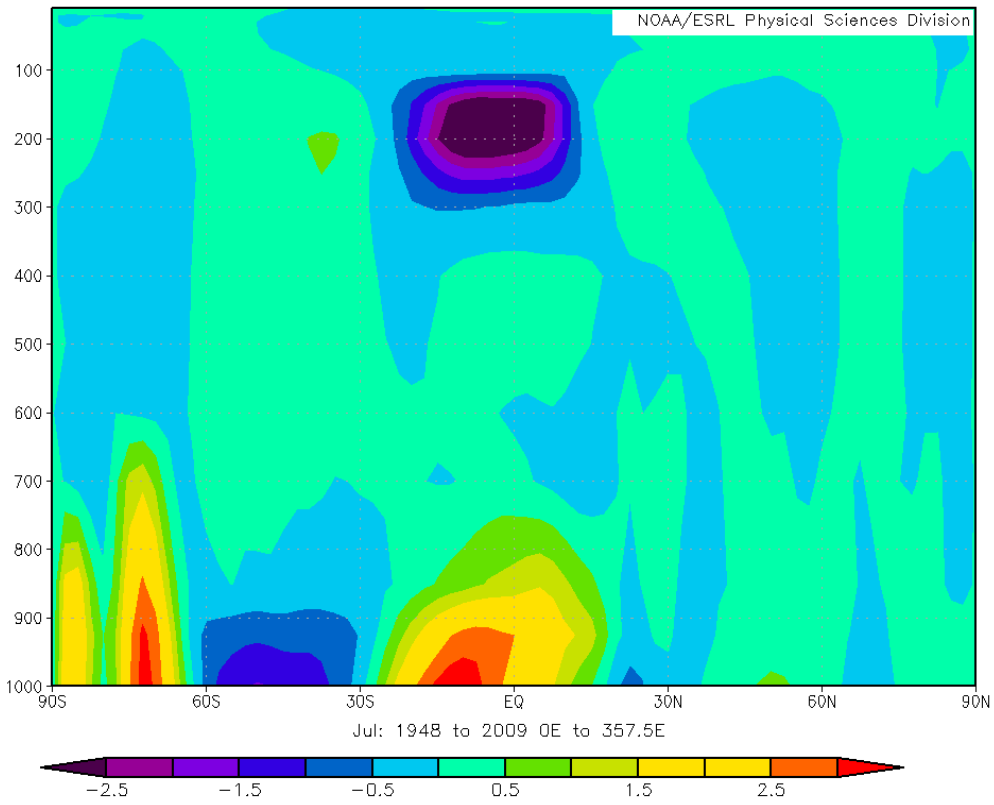

Figure 7: Zonally-averaged zonal velocity data (in units of m/s) are plotted in a latitude-height profile. These data represent a climatological average for the month of July over the years 1948-2009 (ESRL).

2.2 Discussion of climatological Hadley cell data

Several of the expected results concerning the Hadley circulation are displayed by this data. In the temperature plot (Fig. 3), the horizontal temperature contours between about 25°S and 25°N indicate that the Hadley circulation is very effective in homogenizing temperatures in the tropics. This plot also shows a zonal wind distribution consistent with that which is expected. Zonal winds are near zero in the region of upwelling, which in this case is located a few degrees south of the equator, due to the fact that this profile is taken in January, in southern summer. There are also strong upper level jets at the latitudes at which the Hadley circulation subsides, at about 30°N and a few degrees more poleward in the south. Finally, as expected, these upper level westerly jets are associated with sharp horizontal temperature gradients, as each jet is situated over an area in which temperature contours are steeply sloped. In this case, a rough estimation of the thermal wind equation

$$\frac{\partial u}{\partial p} = \frac{R}{fp}\left(\frac{\partial T}{\partial y}\right)_p \tag{1}$$

can be made using the simplification

$$\frac{\Delta u}{\Delta p} = \frac{R}{fp}\left(\frac{\Delta T}{\Delta y}\right)_p, \tag{2}$$

where R is the gas constant, and f is the Coriolis parameter. Using this formula, and estimating values for the northern jet as $\Delta u = 40$ m/s, $\Delta p = 800$ hPa, $\Delta T = 25$K, $\Delta y = 3.3 \times 10^6$ m, $p = 600$ hPa, and $\phi = 30°$, the equation is evaluated as

$$5 \times 10^{-4}\text{ms}^{-1}\text{Pa}^{-1} = 4.97 \times 10^{-4}\text{ms}^{-1}\text{Pa}^{-1}. \tag{3}$$

Therefore, the westerly jets associated with the Hadley circulation are found to be quite consistent with thermal wind balance.

In the plots of vertical velocity, the areas of upwelling and downwelling associated with Hadley cells can be observed. Since this vertical velocity term ω is with respect to pressure surfaces, negative values of ω represent upward motion, while positive values represent downward motion. In each of the vertical velocity plots in Figs. 4 and 5, a large area of negative ω is present near the equator, meaning there is a great deal of upwelling in this equatorial region. It is also worth noting that the area of upwelling is centered on the side of the equator where the season is summer, as it is located at about 5°S in January, and 10°N in July. On either side of this zone of upwelling are zones of downwelling, the locations of which coincide with the edges of the Hadley circulation. The stronger area of downwelling appears to be located in the winter hemisphere. These columns of strong vertical motion are consistent with the expected vertical motions of the Hadley circulation.

Finally, in the plots of meridional velocity shown in Figs. 6 and 7, the expected horizontal components of Hadley circulation are present. Fig. 6 shows a strong poleward velocity in the northern hemisphere in northern winter just below the tropopause, with a strong equatorward velocity at the surface below it. The same effect is observed at a lesser magnitude in the southern hemisphere. Meanwhile, in southern winter, as shown in Fig. 7, the meridional velocities in the southern hemisphere are very much stronger, although the overall pattern is the same.

Through all of these figures, the expected Hadley cell structure is observed, with strong upwelling on the side of the pole on which it is summer, and stronger meridional transport in the hemisphere in which it is winter.

2.3 Low-rotation tank experiment

2.3.1 Methods

To investigate the low-latitude circulation in the lab, an experiment was performed in which a rotating tank was spun at a low rotation rate. The low rotation rate of the tank creates a situation analogous to that of low latitudes on the Earth, at which the effects of the Earth's rotation are not strongly felt. In this experiment, a cylindrical metal container holding ice was placed at the center of the tank. Here, the ice is analogous to the colder mid-latitude atmosphere, while the edge of the tank is analogous to the warm equatorial region.

Before introducing water to the tank, temperature sensors were taped onto the inside of the tank. Two sensors were taped to the edge of the tank, and two sensors were taped to the metal cylinder at roughly the same heights. The sensors were taped in such a way that they did not directly contact the walls of the tank or the cylinder. A fifth sensor was taped to the bottom of the tank about halfway between the cylinder and the outer wall. Water was then added to the tank such that all of the temperature sensors were submerged, and it was spun up to about 0.8 RPM, and allowed to reach solid body rotation.

Once solid body rotation was achieved, ice was introduced to the metal cylinder at the center of the tank, thus causing circulation to begin within the tank. At this time, small paper particles were introduced to the surface of the fluid at various radii from the center of the tank. The motions of these particles were then tracked using Particle Tracker software. After sufficient particle track data had been retrieved, colored dye and permanganate crystals were introduced to the water for a visual representation of the circulation.

The particle position and temperature data were then exported to MATLAB for analysis.[1] The position of the center of rotation of the particles was determined by averaging the

[1]The raw data from Particle Tracker gives particle positions in terms of x and y pixels. In MATLAB, an image of a ruler was used to calculate the pixel to cm conversion scale. The particle positions were then converted to cm.

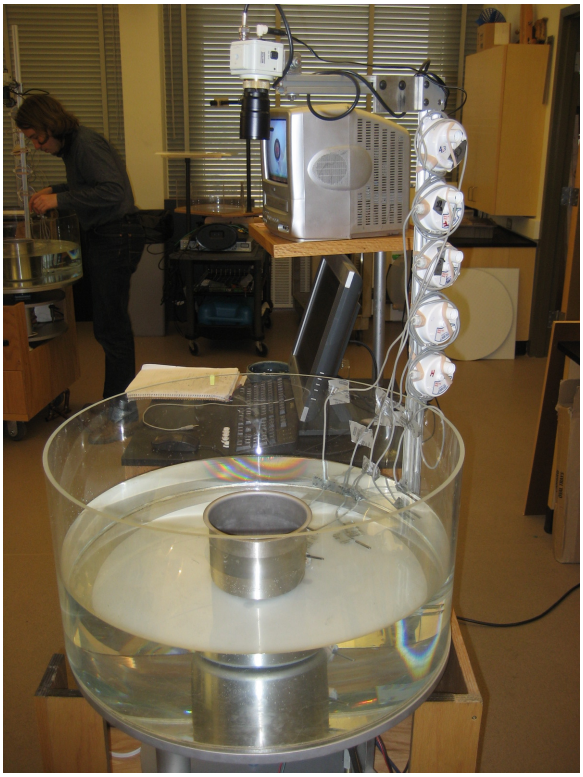

Figure 8: Setup of the lab experiments. The metal cylinder at the center of the tank is filled with ice. The grey wires on the right side of the tank are connected to temperature sensors.

positions of particles for each track, and for each position a radius and an azimuthal velocity was calculated.

2.3.2 Results of the low-rotation experiment

For the low rotation rate experiment, a plot of the particle paths was generated, as well as a plot of all particle azimuthal velocities, and a plot of mean velocities for each particle track. Fig. 9 shows the particle paths, while Fig. 10 shows all observed velocities, and Fig. 11 shows the mean velocities for each path. Photographs of the experiment are shown in Figs. 12 and 13.

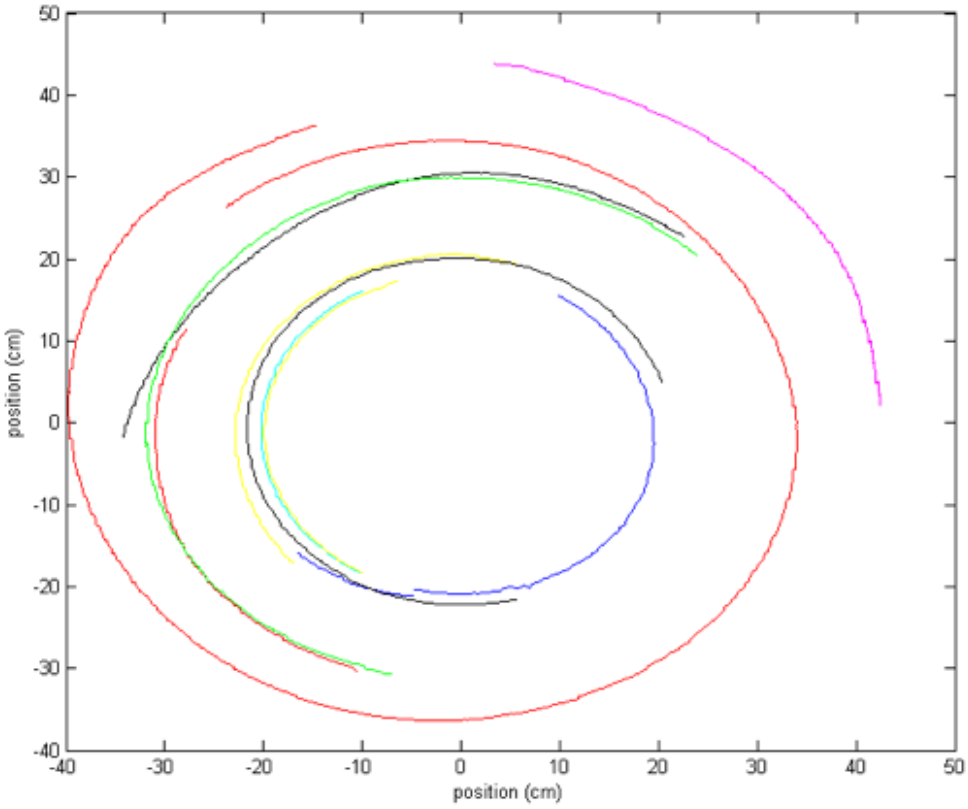

Figure 9: Tracks for each of the particles in the low-rotation experiment. Particle positions are given in cm from the center of rotation.

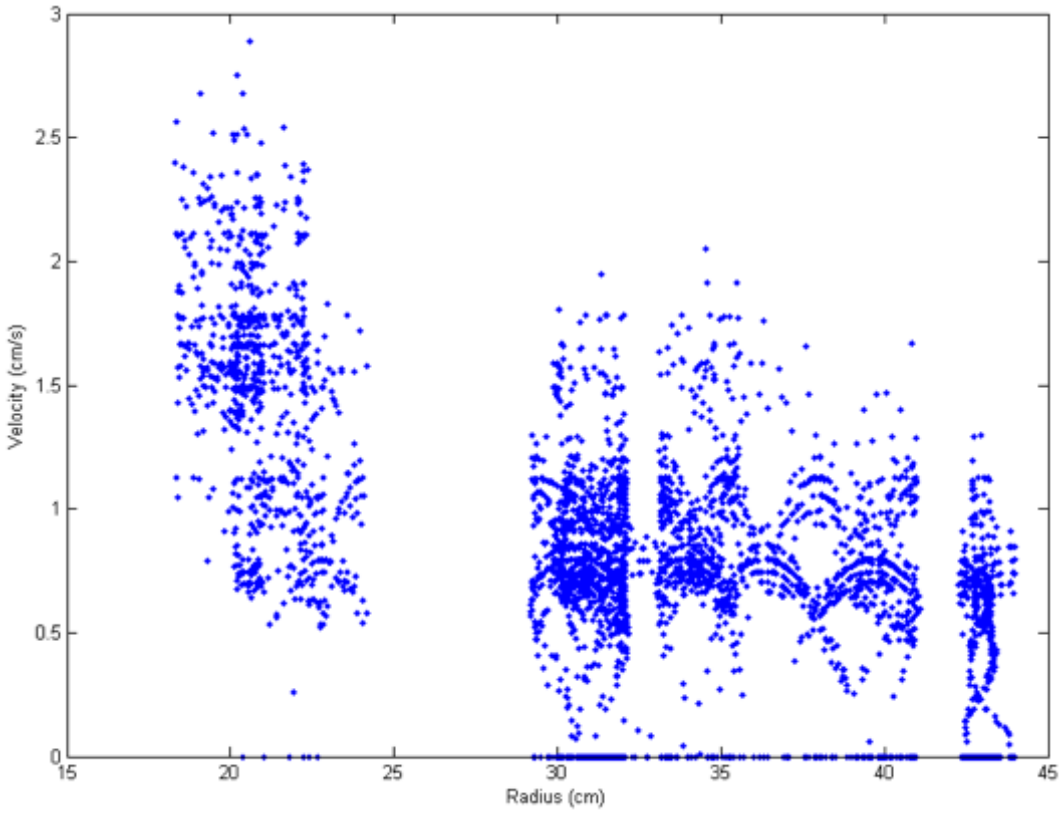

Figure 10: The calculated azimuthal velocities, in cm/s, for each particle position are plotted versus particle radius.

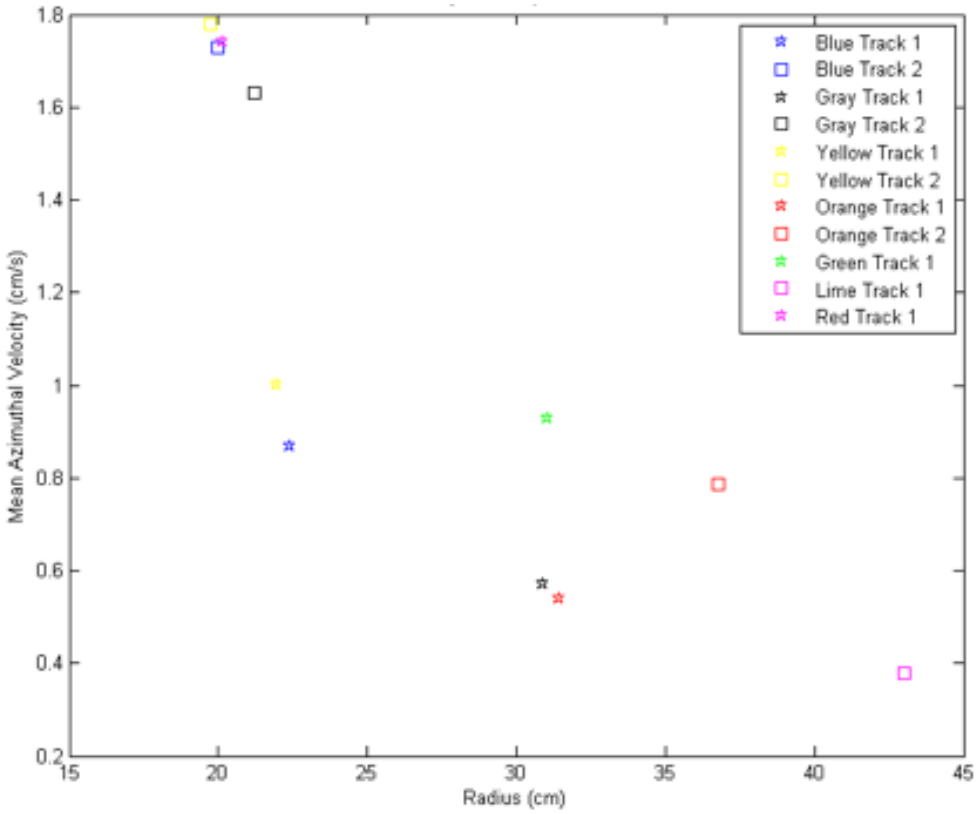

Figure 11: The mean calculated azimuthal velocities, in cm/s, for each individual particle track are plotted versus particle radius.

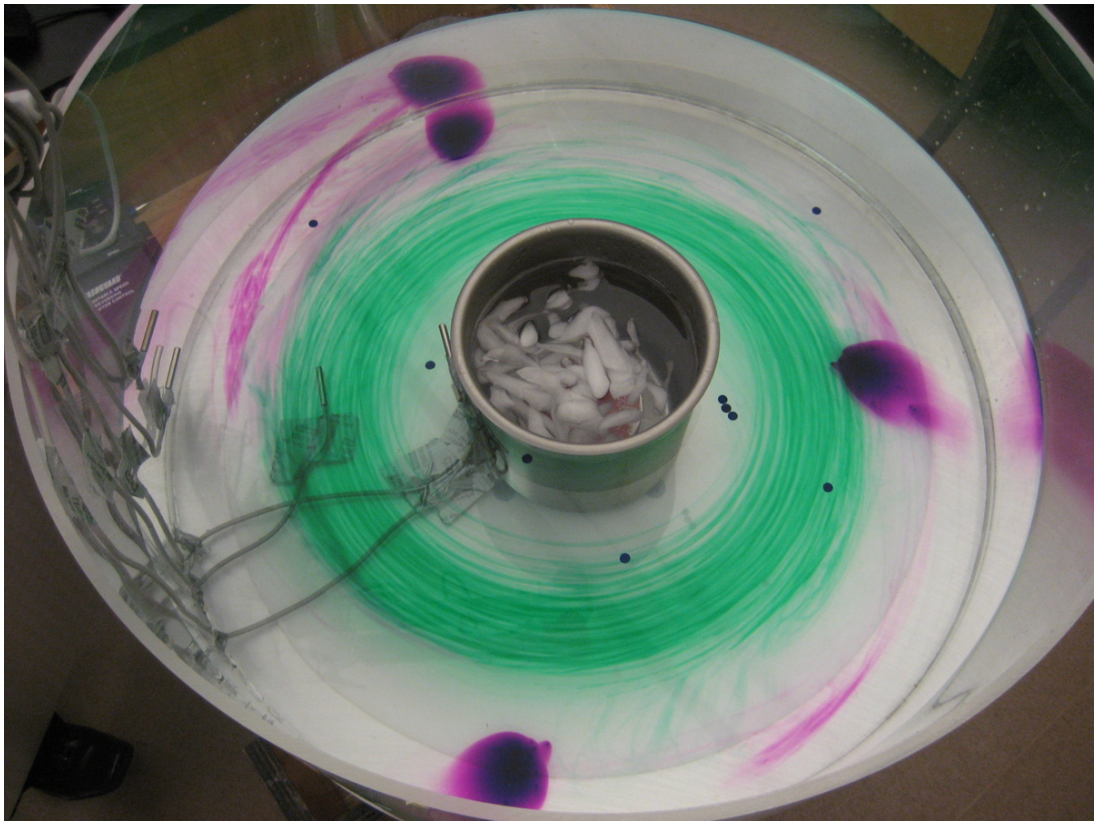

Figure 12: A photograph of the low-rotation experiment from above after the insertion of dye and permanganate crystals.

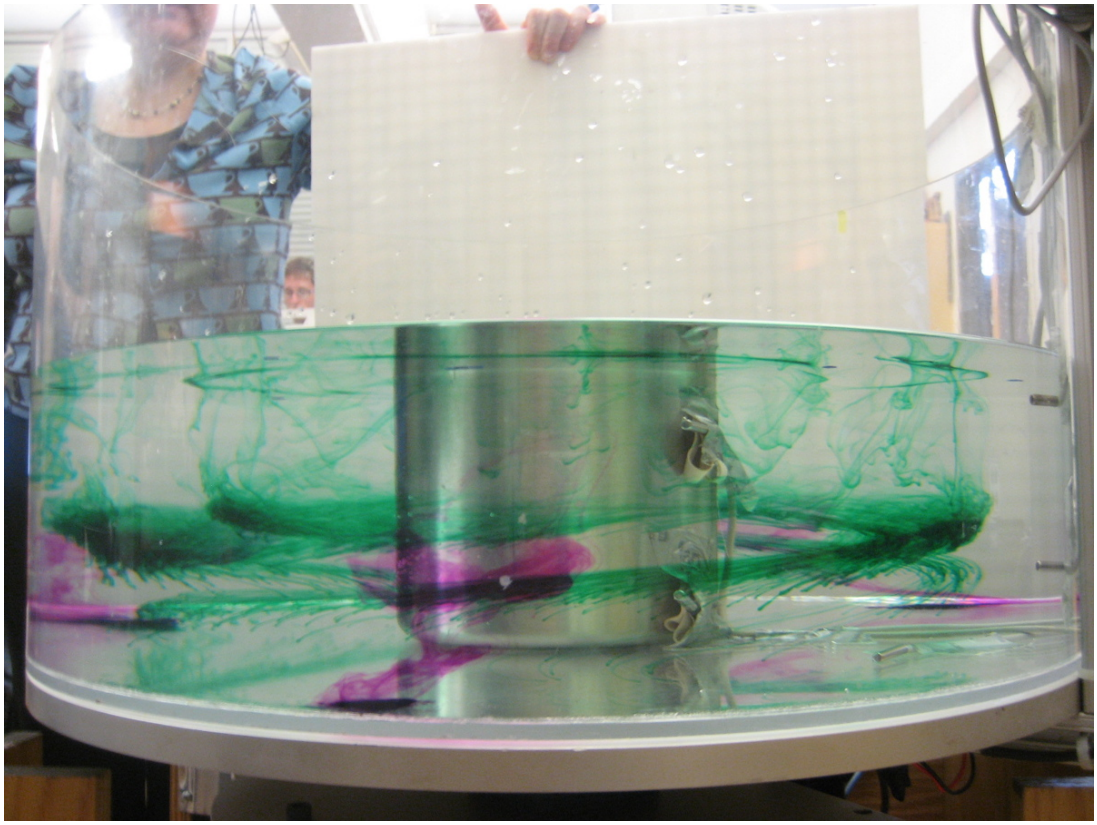

Figure 13: A photograph of the low-rotation experiment from the side after the insertion of dye and permanganate crystals.

Additionally, the thermal wind balance of the fluid was evaluated using the discrete form of the thermal wind equation

$$u(r) = \frac{-\alpha g H}{2f}\left(\frac{\Delta T_1}{\Delta r} + \frac{\Delta T_2}{\Delta r}\right), \tag{4}$$

where α is the coefficient of expansion of water, H is the height of the fluid, ΔT_1 and ΔT_2 are the differences in temperature between inner and outer sensors at the top and bottom of the fluid, and Δr is the distance between inner and outer radii of the fluid. Using this equation and temperature data from the probes used in the experiment, the predicted thermal wind was found to be 1.48 cm/s.

2.4 Discussion of low-rotation experimental results

The observed particle tracks in this experiment show roughly circular motions about a center of rotation. This is consistent with the idea of large-scale radial circulation in which warm water rises at the edge of the tank and moves inward along the surface, gaining azimuthal velocity as it nears the center. Indeed, the particles were found to be moving radially inward to some degree as they progressed azimuthally.

Likewise, as the particles near the cold center of the tank, their azimuthal velocities increase, as shown in the azimuthal velocity plot versus radius presented in Fig. 10. The presence of increased azimuthal velocities at inner radii is consistent with a counterclockwise jet on the surface of the fluid near the location at which cold water sinks at the edge of the ice container. This counterclockwise jet is analogous to the westerly jets found at the poleward edges of the Hadley circulation.

Furthermore, the distribution of azimuthal data in Figs. 10 and 11 suggests that velocity has a relationship with radius which goes as $\frac{1}{r}$. This relationship is consistent with conservation of angular momentum, as particles gain azimuthal velocity when moving radially inward toward the center of rotation of the tank.

Thermal wind was also found to be quite consistent with the flow in the experiment, as the expected jet speed calculated from thermal wind using temperature data was relatively close to the observed jet speed. While the calculated jet speed was 1.48 cm/s, the highest mean azimuthal velocity for a given particle was slightly below 1.8 cm/s. These figures are easily within an order of magnitude, and so the fluid in the experiment can be said to be in thermal wind balance.

In the experiment photos in Figs. 12 and 13, the shear of the flow is visible in the green dye, as the surface jets transport the dye further counterclockwise near the surface. Furthermore, the return flow of the circulation is made visible at the bottom of the tank by the permanganate crystals. The crystals are shown flowing clockwise and outward. This is

analogous to easterly tradewinds, which flow equatorward at the Earth's surface (the bottom of the atmosphere).

3 Mid-latitudes: Atmospheric eddies

While the Hadley circulation is effective in creating heat flux out of the tropics, it typically only extends to latitudes of about 30 degrees. In fact, it would be impossible for a Hadley cell to reach the pole, since conservation of angular momentum would dictate an infinite zonal velocity for tropical air traveling meridionally to the pole. Instead, the effects of the Earth's rotation prohibit large-scale meridional circulation at mid-latitudes, and eddies are formed. These eddies, which are manifested as transient storm systems, are formed as a result of baroclinic instability in the mid-latitude atmosphere. Through baroclinic instability, eddy growth can occur when atmospheric potential energy is released through poleward transport of warm air and equatorward transport of cold air. Thus, while mid-latitude eddies do not feature large-scale meridional transport of warm air, the average heat flux associated with the storms is in the poleward direction. This heat flux can be measured with the transient heat flux quantity $\overline{v'T'}$. Analysis of this quantity in atmospheric data quantifies the heat transport conducted by mid-latitude eddies.

3.1 Climatological transient heat flux data analysis

To investigate the heat transfer effected by mid-latitude eddies, long-term mean climatological transient heat flux data was analyzed for the month of January. The transient heat flux, $\overline{v'T'}$, was integrated in several directions, and the results were plotted.

Fig. 14 shows the zonally averaged transient heat flux, in profile view from south to north pole versus height. Fig. 15 shows the vertically integrated heat flux over the Earth's surface plotted with coastlines. Finally, Fig. 16 shows the vertically integrated zonally averaged heat flux versus latitude.

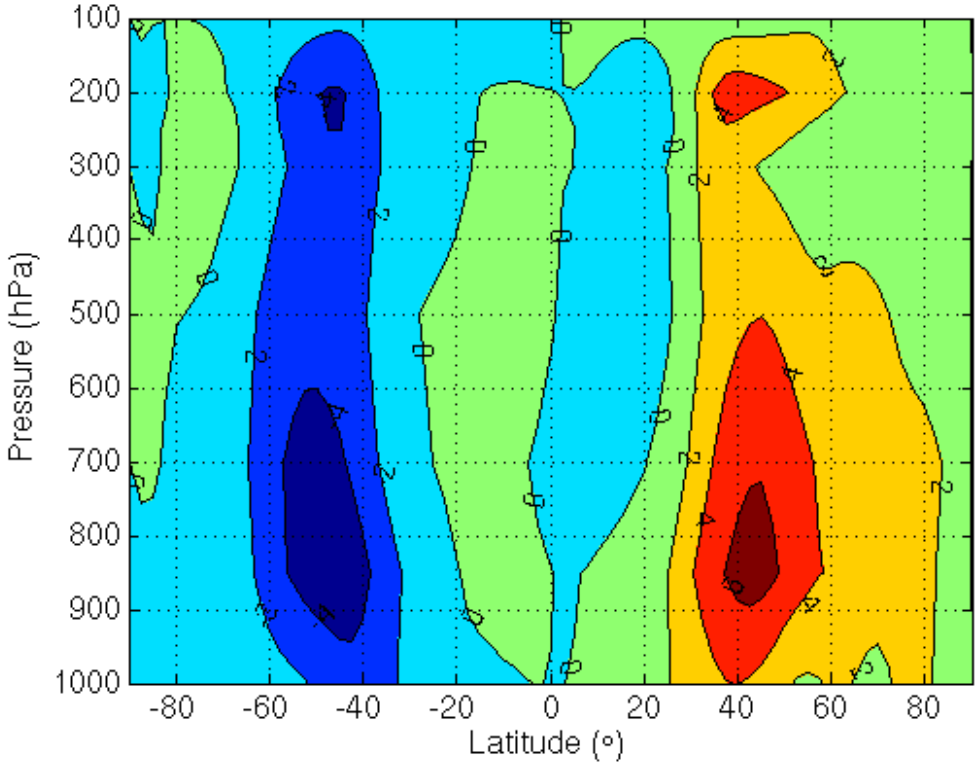

Figure 14: Zonally-averaged transient heat flux for the month of January in a latitude versus height profile. Transient heat flux is shown in units of K m/s.

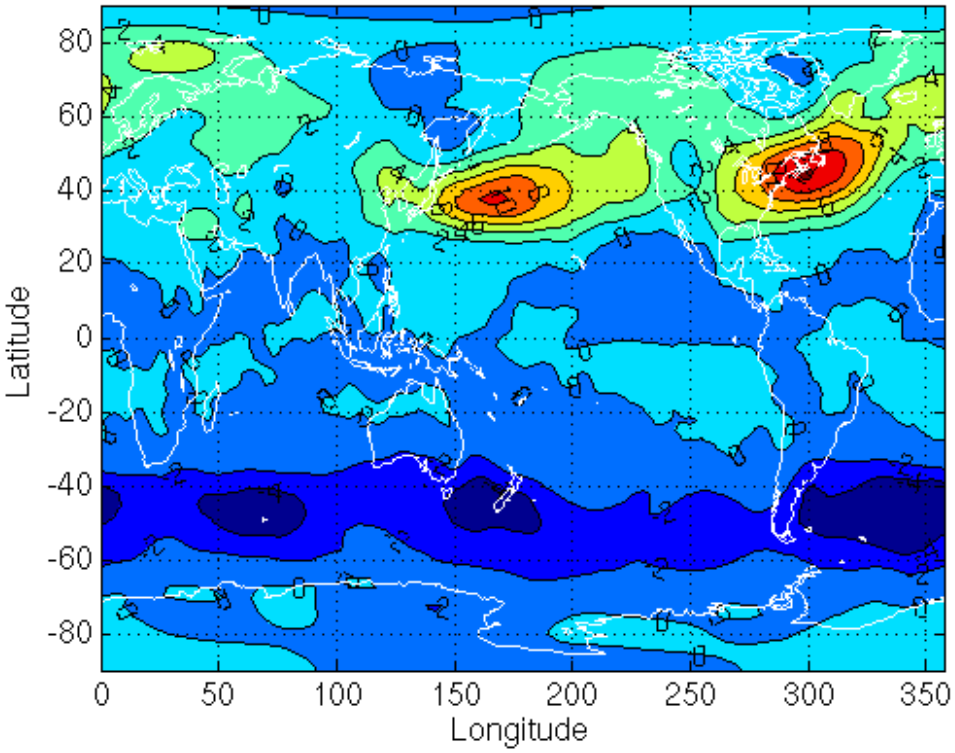

Figure 15: Vertically integrated transient heat flux for the month of January in units of K m/s.

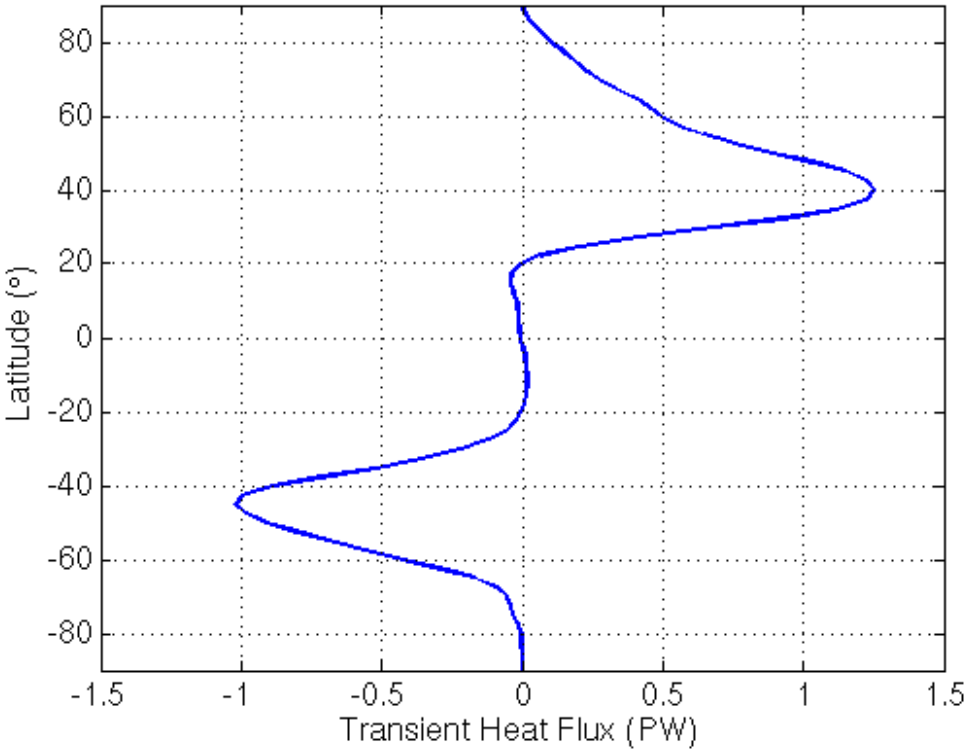

Figure 16: Vertically integrated zonally averaged transient heat flux for the month of January plotted versus latitude in units of K m/s.

3.2 Discussion of climatological transient heat flux data

The transient heat flux data analyzed here present many of the expected results concerning heat flux associated with mid-latitude eddies. The zonally averaged transient heat flux presented in Fig. 14 shows the distribution of meridional heat flux over latitude. As expected, the transient heat flux is relatively low in the tropical regions and near the poles, while its values have large magnitude at mid-latitudes, at around 45° N and S. This is the latitudinal location of baroclinic eddies, indicating that this heat flux is likely associated with these mid-latitude storms. Another important feature is that the meridional transient heat flux is positive at mid-latitudes in the northern hemisphere, while it is negative at the same latitudes in the southern hemisphere. Therefore, the heat transport effected by the mid-latitude atmospheric eddies is poleward in both cases. Finally, while transient heat flux is large at all heights at mid-latitudes, it maximum values are found lower in the atmosphere, at levels around 800 hPa. Since mid-latitude storms operate primarily in the lower atmosphere, this further supports the idea that these storms are responsible for the observed meridional heat transport.

The large magnitude of transient heat flux at mid-latitudes is again evidenced by the vertically integrated transient heat flux data presented in Fig. 15. Again, the values of transient heat flux are relatively low in the tropics and at the pole, while large poleward values are found at mid-latitudes. Furthermore, the locations of maximum transient heat flux are consistent with typical mid-latitude storm tracks. This is again consistent with the fact that poleward heat flux is associated with mid-latitude baroclinic eddies. The larger magnitude of transient heat flux in the northern hemisphere compared to the southern hemisphere is consistent with the fact that this data reflects the situation of northern winter.

Finally, the vertically integrated zonally averaged transient heat flux data shown in Fig. 16 reinforces the fact that transient heat flux is maximized at mid-latitudes, as there are large peaks of transient heat flux at about 40° in either hemisphere. While the magnitude of the poleward heat flux is again larger in the northern hemisphere due to the fact that the data reflects northern winter, there is a maximum value of over 1 petawatt in both hemispheres. Therefore, while there are other processes that transport heat from equator to pole, mid-latitude eddies are responsible for a significant portion of the total poleward heat flux.

3.3 High-rotation tank experiment

3.3.1 Methods

To investigate the mid-latitude circulation in the lab, an experiment was performed in which a rotating tank was spun at a relatively high rotation rate. Since at mid-latitudes, the effects

of the Earth's rotation are significantly felt, the higher rotation rate of the tank creates a situation analogous to that of mid-latitudes on the Earth. In this experiment, a cylindrical metal container holding ice was placed at the center of the tank. Here, the ice is analogous to the colder polar atmosphere, while the edge of the tank is analogous to the atmosphere of the warmer tropical region, and the fluid in between is analogous to that in the mid-latitude atmosphere.

Before introducing water to the tank, temperature sensors were taped onto the inside of the tank. One sensor each was taped to the edge of the tank and to the metal cylinder at roughly the same height. The sensors were taped in such a way that they did not directly contact the walls of the tank or the cylinder. The three remaining sensors were taped to the bottom of the tank at varying radii between the cylinder and the outer wall. Water was then added to the tank such that all of the temperature sensors were submerged, and it was spun up to about 12 RPM, and allowed to reach solid body rotation. The basic setup of the experiment was similar to that shown in Fig. 8.

Once solid body rotation was achieved, ice was introduced to the metal cylinder at the center of the tank, thus causing circulation to begin within the tank. At this time, small paper particles were introduced to the surface of the fluid at various radii from the center of the tank. The motions of these particles were then tracked using Particle Tracker software. After sufficient particle track data had been retrieved, colored dye was introduced to the water for a visual representation of the circulation. Additionally, the time taken for the ice in the metal cylinder to melt was recorded. The particle position and temperature data were then exported to MATLAB for analysis.

3.3.2 Results of the high-rotation experiment

For the high rotation rate experiment, a plot of the particle paths was generated, as well as a plot of the observed temperatures at each sensor over the course of the experiment. Fig. 17 shows the particle paths, while Fig. 18 shows the observed temperature data. A photograph of the experiment is shown in Fig. 19.

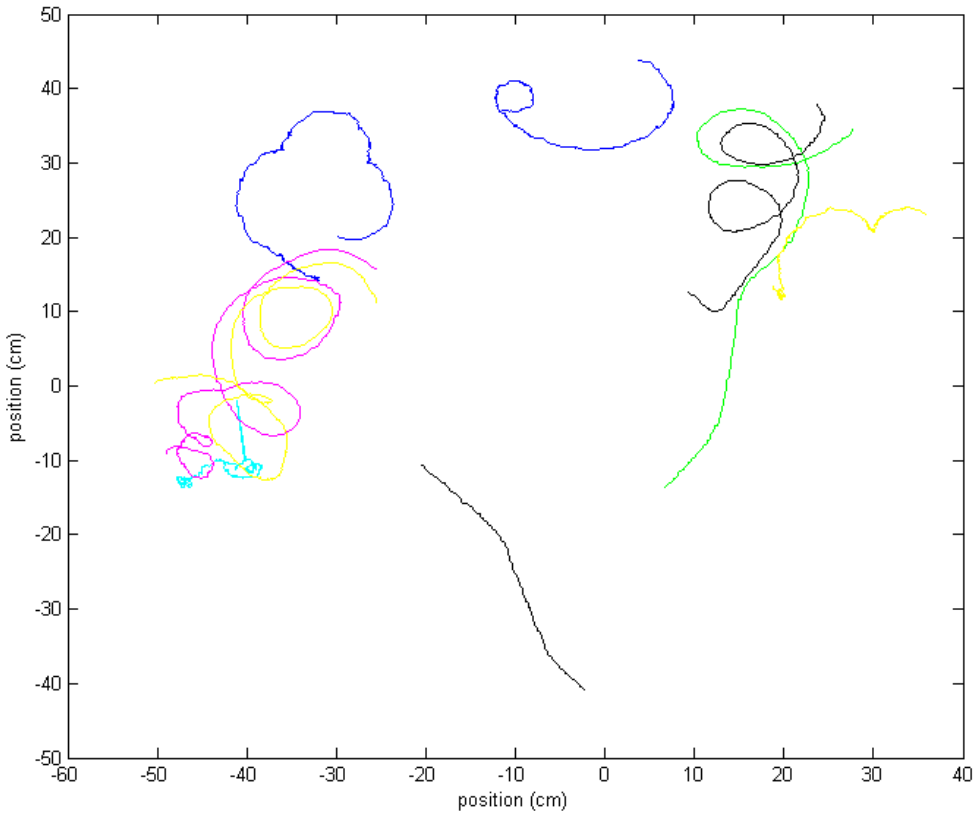

Figure 17: Tracks for each of the particles in the high-rotation experiment. Particle positions are given in cm from the center of rotation.

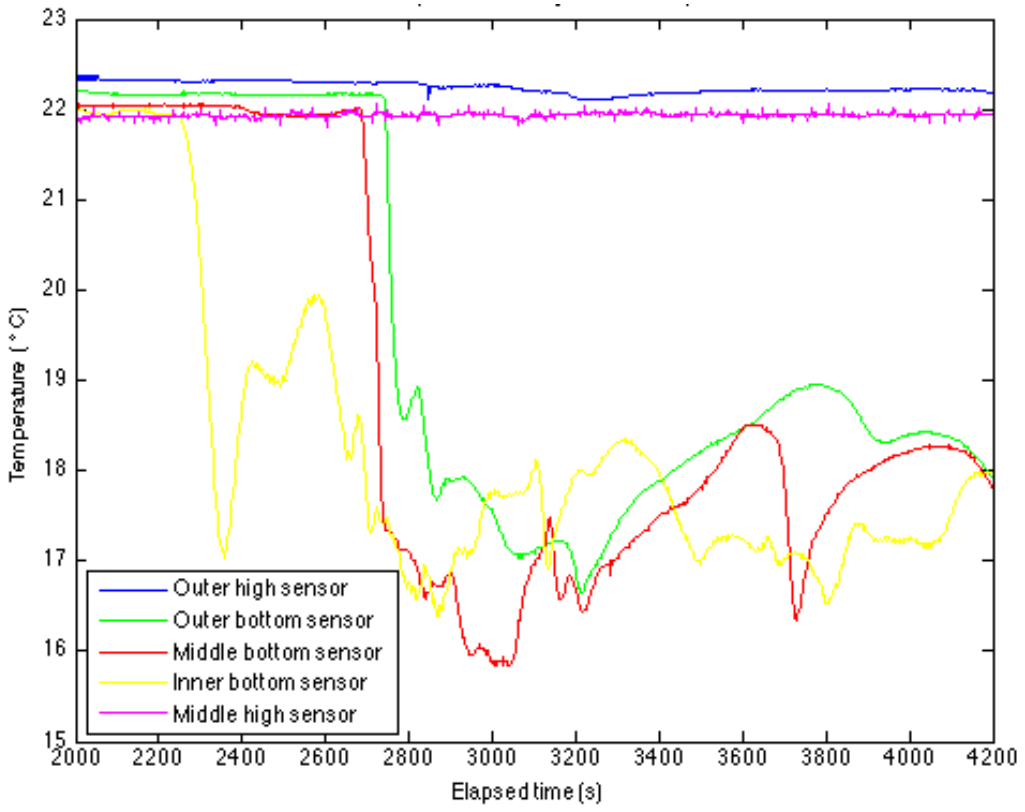

Figure 18: The observed temperatures, in °C, for each temperature sensor are plotted versus time for the duration of the experiment.

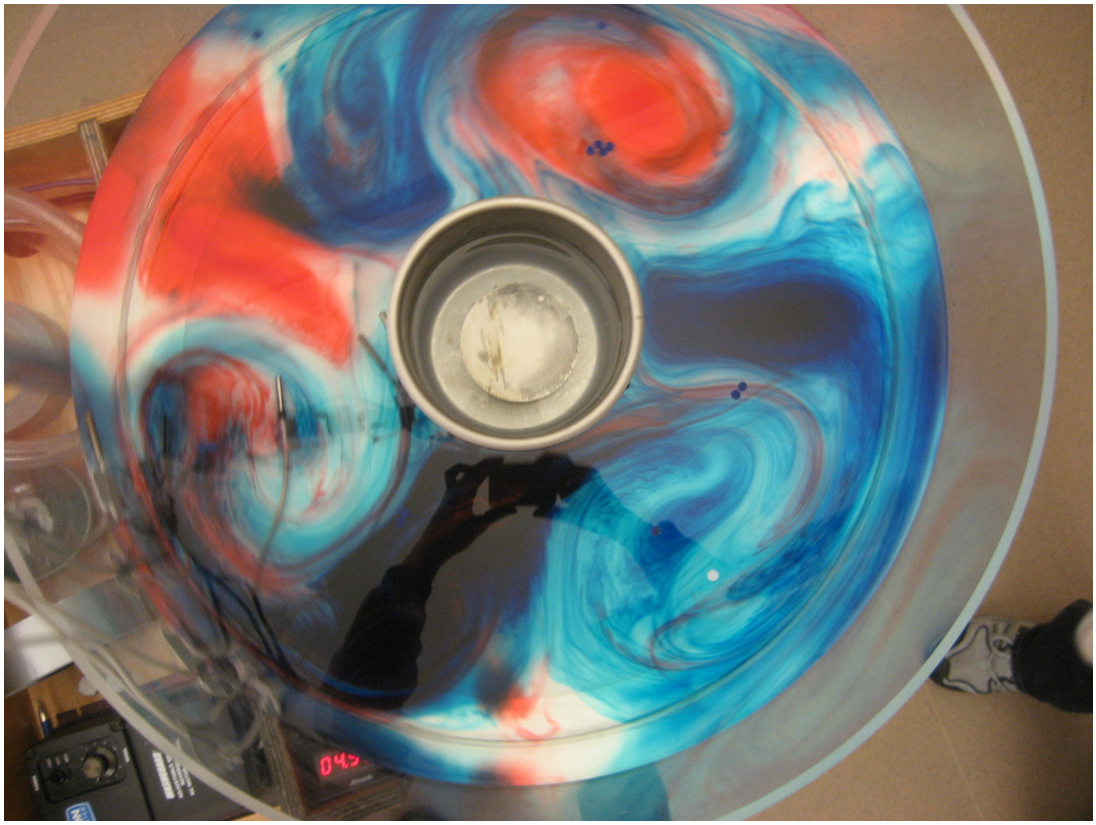

Figure 19: A photograph of the high-rotation experiment from above after the insertion of dye.

Additionally, the heat flux balance of the fluid was evaluated using the equation

$$L\frac{\Delta m}{\Delta t} = 2\pi r \rho c_l \int_0^H [\overline{v'T'}]dz, \tag{5}$$

where L is the latent heat of fusion of ice, Δm is the mass of ice used, Δt is the time required for all of the ice to melt, r is a representative radius, in this case chosen to be halfway between the metal cylinder and the edge of the tank, ρ is the density of water, and c_l is the specific heat capacity of water. Here, the left side of the equation represents the heat flux required to melt the ice in the metal cylinder, while the right side represents the radial heat flux for which the eddies formed in the tank are responsible, calculated using temperature and velocity variance data. For the left side of the equation, the calculated heat flux was 144 watts. Meanwhile, temperature variance data from the top and bottom of the fluid were used to create a range for the right hand side of the equation. With bottom temperature data, heat flux due to the eddies was calculated to be 2348 watts, while top temperature data yielded a figure of 1.3 watts.

3.4 Discussion of high-rotation experimental results

The observed particle tracks in this experiment show turbulent flow on the surface of the fluid. Instead of large, circular paths, in which the particles revolve around the center of the tank, the particles traced out spiral-like patterns, and did not progress around the entire tank. These spiral motions are consistent with eddy flow, which was present in the tank. It was also observed that while there was no obvious preferred direction for particles to travel, the several of the particles seemed to spiral in a direction that was generally counter-clockwise around the tank. This is analogous to the mid-latitude atmosphere, in which baroclinic eddies travel westward.

The temperature data collected from the five sensors in the tank also exhibited signs of turbulent flow. While each of the temperature sensors was originally at approximately the same temperature level, the bottom temperature sensors recorded a sharp drop in temperature as eddy flow brought cold water from inner radii progressively over each one. From this point forward, the bottom sensors showed greatly varying temperatures consistent with turbulent flow. In contrast, the top sensors showed very little variation in temperature throughout the experiment. This is likely due to the fact that the top of the fluid was in thermal contact with surrounding air, thereby limiting the magnitude of temperature fluctuations at the top of the fluid.

The heat flux budget conducted found the calculated flux into the ice container and the total calculated eddy heat transport to differ by an order of magnitude. The calculated value of heat flux into the ice container was 144 watts, while the eddy heat transport was

found to be 2348 watts when calculated using temperature data from the bottom of the tank. However, the heat flux into the container in the center of the tank should be an upper bound for eddy heat flux, since in actuality some of the energy required to melt the ice likely came from the surrounding air, and not necessarily from the surrounding water. Therefore, assuming the figure of 144 watts to be correct, the calculated figure of 2348 watts is an overestimate of the actual eddy heat transport.

This overestimate could be due to the fact that correlation of temperature and velocity perturbations was not taken into account. The original calculation assumes that all positive values of v' (radially inward transport) were associated with positive values of T' (warm water transport). However, this was likely not the case, and a correlation coefficient would likely have to be introduced to correct for this error. For instance, if a correlation coefficient of 0.2 were used, the calculated eddy heat flux would be reduced to 470 watts.

The estimate of eddy heat flux is further reduced when considering that the heat transport was not constant throughout the height of the fluid. The current calculation assumes vertical homogeneity when integrating over the height of the fluid. However, this is not the case, as it is observed by the temperature sensors at the top of the fluid that there is almost no radial heat transport there. Therefore, it can be concluded that the actual heat flux for which the eddies were responsible was somewhere between 1 and 470 watts. This is therefore consistent with the figure of 144 watts calculated using the time and energy required to melt the ice.

The experiment photo in Fig. 19, several eddies are made visible in the fluid by the presence of blue and red dye. These eddies show cold water from near the center of the tank being mixed with warm water from the outside edges of the tank.

4 Conclusions

From this study, it can be concluded that the general circulation of the atmosphere is composed of Hadley cell circulations at low latitudes, and of turbulent baroclinic eddies at mid-latitudes. At low latitudes, the weak effects of the Earth's rotation allow for large-scale overturning meridional air circulations. In association with these circulations, upwelling leads to deep convection in equatorial regions, while dry subsidence results in the presence of deserts in the subtropics. This circulation causes meridional temperature gradients to be small within the tropics, but sharp temperature gradients exist at the periphery of the Hadley cells. The strong westerly jets found in the upper atmosphere at the same latitudes as these temperature contrasts are found to be consistent both with thermal wind balance and with conservation of angular momentum with air moving poleward from the equator and closer to the Earth's axis of rotation.

It can also be concluded that while rotational effects prohibit large-scale meridional circulations at mid-latitudes, eddies formed at these latitudes due to baroclinic instability

are able to contribute to poleward transport of warm air. Overall, it is found that the low-latitude Hadley circulation works in concert with mid-latitude eddies to move warm equatorial air poleward, as well as moving cold polar air equatorward. This meridional heat flux is found to lessen the temperature gradient created between pole and equator by differences in solar heating.

The laboratory experiments conducted in this study are concluded to be analogous to phenomena occurring in the general circulation of the atmosphere. The low-rotation experiment creates an overturning radial circulation analogous to the low-latitude Hadley circulation. Likewise, the high-rotation experiment creates eddies analogous to those found at mid-latitudes in the atmosphere. Finally, it is concluded that the heat transport effected by the phenomena in each of these experiments is analogous to the meridional heat flux generated by the general circulation of the atmosphere.

Future studies could examine the poleward heat flux generated by ocean circulations. Another study could examine the degree to which heat is transferred poleward in the atmosphere through latent heat flux associated with moisture and condensation.

5 References

"e-WALL: The Electronic Map Wall" - Dept. of Meteorology, The Pennsylvania State University. http://www.meteo.psu.edu/ gadomski/SAT_NHEM/atlrecentwv.html - Last accessed May 12, 2009

Illari, Lodovica; Marshall, John. April 2009 - "12.307 Project 4: General Circulation"

Marshall, John; Plumb, R. Allen. 2008 - *Atmosphere, Ocean, and Climate Dynamics: An Introductory Text.* Elsevier.

"Monthly/Seasonal Climate Composites" - NOAA Earth System Research Laboratory Physical Sciences Division. http://www.cdc.noaa.gov/cgi-bin/data/composites/printpage.pl - Last accessed May 14, 2009